Cyclin A2 localises in the cytoplasm at the S/G2 transition to activate Plk1

Helena Silva Cascales[1], Kamila Burdova[2], Erik Müllers[1#], Henriette Stoy[1], Patrick von Morgen[2], Libor Macurek[2], Arne Lindqvist[1*]

*Corresponding author:
Arne Lindqvist
Department of Cell and Molecular Biology
Karolinska Institutet
Stockholm, Sweden
Phone: +46-8-52487309
E-mail: arne.lindqvist@ki.se

Affiliations
1. Department of Cell and Molecular Biology; Karolinska Institutet; Stockholm, Sweden.
Current address: Discovery Sciences, AstraZeneca R&D; Gothenburg, Mölndal, Sweden.
2. Laboratory of Cancer Cell Biology; Institute of Molecular Genetics; Academy of Sciences of the Czech Republic; Prague, Czech Republic.

Running title: Cytoplasmic Cyclin A2 at S/G2 transition

Keywords: Cyclin A2, Plk1, Bora, Cell cycle, DNA damage, Cdk1, Cdk2, p21,

Summary statement

Cyclin A2 localises in the cytoplasm at completion of DNA replication, suggesting a mechanism for coupling S-phase with activation of the mitotic kinase Plk1

Abstract

Cyclin A2 is a key regulator of the eukaryotic cell cycle. By forming complexes with Cdk1 and Cdk2, Cyclin A2 regulates both spatial and temporal phosphorylation of target proteins, particularly during S and G2 phases. Here we describe a change in localisation of Cyclin A2 from being only nuclear to both nuclear and cytoplasmic at the S/G2 border. Inflicting DNA damage in G2 phase led to a complete loss of cytoplasmic Cyclin A2 in a manner that depended on p53 and p21. In the absence of externally induced DNA damage, $p21^{-/-}$ cells showed increased cytoplasmic localisation of Cyclin A2. In addition, depletion of Cdk1 delayed accumulation of cytoplasmic Cyclin A2, suggesting that the combined action of Cdk1 and p21 can modulate Cyclin A2 localisation. Interestingly, Cyclin A2 localisation change occurs simultaneously with Plk1 kinase activation, and we provide evidence that cytoplasmic Cyclin A2 can activate Plk1. We propose that cytoplasmic appearance of Cyclin A2 at the S/G2 transition could function as the long sought for trigger for mitotic kinase activation.

Introduction

Correct progression through the cell cycle depends on the tight regulation of Cyclin-Cdk complexes over time. Sequential waves of Cyclin dependent kinase (Cdk) activity ensure timely phosphorylation of a large amount of substrates. Cyclins are key elements to provide target specificity and affinity to Cdks. Both Cyclin A2 (CycA2) and Cyclin B1 (CycB1) have been widely studied due to their involvement in progression from S phase through G2 and mitosis (Morgan, 2007). However, the specific functions and regulation of CycA2 still remain largely unknown.

Lack of CycA2 leads to early embryonic lethality, suggesting a critical role for CycA2 in cell cycle regulation (Kalaszczynska et al., 2009; Liu et al., 1998; Murphy et al., 1997). Due to its presence during S, G2, and early mitosis, CycA2 is at a strategic position to control a large part of the cell cycle (Fung et al., 2007; Pagano et al., 1992; Woo and Poon, 2003). Whereas CycA2 predominately associates with Cdk2 during S phase, association with Cdk1 increases during the late cell cycle, suggesting that CycA2 can play multiple roles depending on cell cycle stage (Merrick et al., 2008). Indeed, CycA2 regulates multiple aspects of S-phase, including phosphorylation of the prereplication complexes (Furuno et al., 1999; Katsuno et al., 2009), phosphorylation of components of the replication machinery (Cardoso et al., 1993; Frouin et al., 2005), and phosphorylation of Cdc6 to prevent re-replication (Petersen et al., 1999). However, depletion of CycA2 primarily leads to an arrest in G2 phase, suggesting that progression through G2 phase is a key function for CycA2 (Bloom and Cross, 2007; De Boer et al., 2008; Fung et al., 2007; Gong and Ferrell, 2010; Gong et al., 2007; Oakes et al., 2014).

During G2 phase, CycA2 stimulates transcription and represses degradation of multiple mitotic regulators (Hein and Nilsson, 2016; Laoukili et al., 2008; Lukas et al., 1999; Oakes et al., 2014). As the mitotic regulators accumulate, CycA2 participates in the feedback-loops that culminate in full CycB1-Cdk1 activation and mitotic entry (Mitra and Enders, 2004). A key player in these feedback-loops is Polo-like kinase 1 (Plk1) (Lindqvist et al., 2009). Plk1 requires Cdk-mediated phosphorylation of the co-factor Bora for activation, and both CycA2- and CycB1-containing complexes have been suggested to phosphorylate Bora (Gheghiani et al., 2017; Parrilla et al., 2016; Thomas et al., 2016).

As CycA2 functions in both S and G2 phases, how S-phase and G2-phase targets are temporally separated remains unclear. Interestingly, although at least S-phase CycA2 targets are predominately nuclear, CycA2 has been shown to regulate events in the cytoplasm. This includes G2 roles as loading Eg5 to centrosomes (Kanakkanthara et al., 2016) and inhibiting endocytic vesicle fusion to control membrane transport as cells enter into mitosis (Woodman et al., 1993). Recently, CycA2 has been reported to regulate cell motility and invasiveness by interacting with RhoA (Arsic et al., 2012; Bendris et al., 2014). Thus, CycA2 has both nuclear and cytoplasmic functions.

Despite being predominantly nuclear and not possessing a classical NLS, CycA2 is known to shuttle between the nucleus and cytoplasm to act on both nuclear and cytoplasmic substrates (Jackman et al., 2002). In turn, CycA2 association with different proteins may affect localisation both to the nucleus and to the cytoplasm (Maridor et al., 1993; Tsang et al., 2007). However the exact mechanism that regulates CycA2 localisation remains elusive.

In order to study the localisation of Cyclin A2 in the human cell cycle we used gene-targeting to create a fusion between Cyclin A2 and YFP. Here we describe the cell cycle-dependent localisation of CycA2 in the cytoplasm at the S/G2 transition. We further describe that cytoplasmic localisation of CycA2 is abolished in response to DNA damage in a manner that depends on p21. Although our data indicate that additional modes of regulation likely exist, we show that Cdk1 and p21 can act in a collaborative manner to modulate CycA2 localisation. Finally, we show that CycA2 interacts with Bora in the cytoplasm and contributes to Plk1 activation at the S/G2 transition.

Results

Cyclin A2 accumulates in the cytoplasm at the S/G2 transition

In order to study the dynamics of CycA2 in live cells we targeted *CCNA2* using rAAV-mediated homologous recombination. We introduced an ORF for EYFP in the *CCNA2* locus of U2OS (Akopyan et al., 2014) and RPE cell lines to create a CycA2-eYFP fusion protein (Figs. 1A and S1A,B). Western blot analysis confirmed the successful integration of the EYFP ORF in one of the two alleles of CycA2 as we detected a band that migrated at the predicted size of endogenous untagged CycA2 and a band that migrated at the predicted size of the CycA2-eYFP fusion protein (Fig. S1A). Importantly, siRNA to target CycA2, addition of S-trityl-L-cysteine (STLC), or addition of etoposide showed a similar behaviour of both bands as to CycA2 in parental RPE cells, indicating that eYFP was specifically introduced at the *CCNA2* locus (Fig. S1A). As previously described, CycA2-eYFP is present in all cells from the beginning of S phase and its levels increase over time reaching a maximum at mitosis when CycA2 is rapidly degraded (Figs. 1A and S1B) (Akopyan et al., 2014).

Time-lapse imaging of gene-targeted U2OS and RPE cells revealed the presence of CycA2-eYFP in the cytoplasm in all cells before entry into mitosis (Figs. 1A and S1B). We traced individual RPE-CycA2-eYFP cells and quantified the YFP intensity both in the nucleus and the cytoplasm (Fig. 1B). We observed a nuclear CycA2-eYFP increase over time reaching a maximum at mitosis. Interestingly we also observed a dip in the nuclear signal starting 4 to 6 hours before mitosis, concomitant with an increase in the cytoplasmic signal of CycA2-eYFP. The reduction of nuclear CycA2-eYFP when cytoplasmic CycA2-eYFP appears could indicate that CycA2 is translocated from the nucleus to the cytoplasm. Nonetheless, both the nuclear decrease and the cytoplasmic increase of CycA2-eYFP were consistent in all cells that entered mitosis, indicating that CycA2-eYFP localisation change is a cell cycle regulated event (Fig. 1B).

In order to pinpoint the position in the cell cycle when cells start to accumulate cytoplasmic CycA2, we treated RPE CycA2-eYFP cells with a short pulse of EdU to mark cells in S phase and stained with antibodies against GFP to detect CycA2-eYFP and DAPI to measure the DNA content. Quantification of the stainings showed that whereas CycA2-eYFP is present in the nucleus from early S-phase, cells positive for cytoplasmic CycA2-eYFP contain 4n DNA content and low EdU staining, indicating that accumulation of CycA2-eYFP occurs in G2 phase (Fig. 1C). We next performed a similar analysis on parental untagged RPE cells, using an antibody to detect endogenous CycA2. Again, we could observe that the majority of cells positive for cytoplasmic CycA2 show a G2 DNA content and low EdU staining (Fig. 1D). However, we note that CycA2-eYFP showed a slightly higher expression in the cytoplasmic fraction compared to CycA2 (Fig. 1E). Indeed, the presence of an EYFP could alter the dynamics of the endogenous protein (Snapp, 2005). Importantly however, although the magnitude of cytoplasmic accumulation may differ, the timing of cytoplasmic appearance is similar for CycA2 and CycA2-eYFP, showing that CycA2-eYFP can be used to study CycA2 localisation (Figs. 1C,D).

In both parental and CycA2-eYFP RPE cells, a subset of cells containing cytoplasmic CycA2 were positive for EdU, likely reflecting the time difference between EdU addition and fixation of the cells (Figs. 1C,D). This indicates that CycA2 appears in the cytoplasm immediately after completion of S-phase, 4-6h before mitosis (Figure 1B-D). To detect whether cytoplasmic accumulation of CycA2-eYFP depends on completion of S-phase, we treated RPE-CycA2-eYFP cells with thymidine or hydroxyurea and quantified the amount of cells that accumulate CycA2-eYFP in the cytoplasm (Fig. 1F). The treatment with either drug resulted in a decreased number of cells accumulating CycA2 in the cytoplasm, suggesting that cells blocked in S phase do not gain cytoplasmic CycA2-eYFP, further indicating that CycA2-eYFP starts to localise in the cytoplasm at the S/G2 transition.

Cyclin A2-eYFP cytoplasmic appearance after modulation of Cdk activity

The observation that CycA2-eYFP only accumulates in the cytoplasm after S-phase completion suggests that cytoplasmic accumulation is suppressed during S-phase or stimulated during G2 phase. We previously showed that mitotic-inducing activities of Cdk1 and Plk1 start to accumulate at the S/G2 transition (Akopyan et al., 2014). However, we find no evidence that addition of inhibitors to Plk1 or its upstream kinase Aurora A affects cytoplasmic appearance of CycA2 (not shown). Addition of inhibitors to Cdk1 or Cdk2 led to a slight decrease in cells accumulating cytoplasmic CycA2-eYFP, but interpretation of these results is hampered by that Cdk inhibition may affect S-phase progression (not shown). To this end, we followed individual cells that had a low but clear presence of CycA2-eYFP in the cytoplasm at the time of addition of inhibitors. To improve comparison, we synchronised these cells *in silico* at the time point when each cell reaches a certain level of cytoplasmic CycA2-eYFP (Fig. S2A). This allowed us to assess the contribution of Cdk1/2 activity to the cytoplasmic localisation of CycA2-eYFP specifically in G2 phase. We did not observe significant differences in the dynamics of cytoplasmic accumulation of CycA2-eYFP in either of the treatments, showing that a reduction of Cdk1/2 activity does not compromise cytoplasmic accumulation of CycA2-eYFP once initiated (Fig. S2A).

To test if Cdk1/2 activity could promote the onset of cytoplasmic accumulation of CycA2-eYFP, we increased Cdk activity using a Wee1 inhibitor. Wee1 inhibition increased the amount of mitotic cells and decreased the duration between cytoplasmic appearance of CycA2-eYFP and mitotic entry, suggesting that Cdk activity is increased and that G2 phase is shortened. However, we did not detect an increased rate of cytoplasmic appearance of CycA2-eYFP after Wee1 inhibition (Fig. S2B). Thus, although Cdk1/2 activity cannot be excluded as a regulator of CycA2 localisation, other components likely play a more decisive role in this process.

Cdk1 can contribute to cytoplasmic accumulation of Cyclin A2

Given the lack of evidence for key G2 kinase activities to modulate CycA2 localisation, we reasoned that perhaps a change in binding partner could explain CycA2 cytoplasmic localisation. CycA2 is described to complex predominately with Cdk2 in S-phase and increasingly with Cdk1 as cells approach mitosis (Merrick et al., 2008). Furthermore, while Cdk2 is mostly nuclear, Cdk1 is present both in the nucleus and cytoplasm (Moore et al., 1999; Pines and Hunter, 1991, 1994), therefore potentially providing a mechanism to regulate CycA2 localisation.

To investigate the involvement of Cdk-Cyclin complex formation in the localisation of CycA2 we used siRNAs to target either Cdk1 or Cdk2 (Fig. 2A). Live-cell imaging of RPE CycA2-eYFP cells after Cdk1 or Cdk2 knockdown revealed reduced numbers of cells going through mitosis. Further, Cdk1 knockdown increased mitotic duration, showing that knockdown of either Cdk affected cell cycle progression (Fig. 2B). We transfected either Cdk1 or Cdk2 siRNAs for 48 h, fixed cells after treating them with a short pulse of EdU, and stained using CycA2 antibodies and DAPI (Fig. 2C). Analysis of quantitative immunofluorescence in single cells revealed that knock down of Cdk1 led to an increase in the number of cells in G2, presumably due to a lengthening of G2 phase, and subsequently, to the amount of cells with cytoplasmic CycA2 (Fig. 2C,D). Interestingly, a subset of G2 cells contained high nuclear CycA2 and low cytoplasmic CycA2 levels, indicating that Cdk1 may facilitate the localisation of CycA2 to the cytoplasm (Fig. 2C, arrows; Fig. 2D, grey triangle). On the other hand, Cdk2 knockdown led to a marked decrease in number of cells in G2 phase, explaining the reduced level of CycA2 and Cdk1 on a population level (Fig. 2A,C, and D). However, contrary to the observation after Cdk1 depletion, the relation between nuclear and cytoplasmic CycA2 was similar after Cdk2 and control knockdown (Fig. 2D). This suggests that Cdk1 influences the cytoplasmic accumulation of CycA2. We therefore sought to test if Cdk1 binds to cytoplasmic CycA2 and Cdk2 binds to nuclear CycA2. To this end, we immunoprecipitated CycA2-eYFP from cytosolic and nuclear fractions and probed for Cdk1 or Cdk2. We find that although the distribution may differ somewhat, both Cdk1 and Cdk2 are present in both nuclear and cytoplasmic CycA2-eYFP immunoprecipitates (Fig. 2E). Thus, our data suggest that Cdk1 is involved in cytoplasmic localisation of CycA2, but also that cytoplasmic CycA2 exists in complex with Cdk2, showing that cytoplasmic appearance of CycA2 cannot be explained solely by association with Cdk1.

DNA damage response modulates cytoplasmic accumulation of CycA2

We next sought to test if activities present during S-phase retain CycA2 in the nucleus. S phase progression is associated with a low degree of activation of the DNA damage response (Petermann and Caldecott, 2006). We hypothesised that the DNA damage response could directly or indirectly inhibit CycA2 cytoplasmic localisation during S phase. Indeed, addition of Etoposide or Neocarzinostatin, two compounds that cause double strand DNA breaks, resulted in nuclear accumulation of CycA2-eYFP in G2 cells, suggesting that CycA2 localisation is regulated by the DNA damage response (Fig. 3A and not shown). The loss of cytoplasmic CycA2-eYFP was accompanied by an increase in nuclear CycA2-eYFP levels suggesting that upon DNA damage CycA2 is translocated into the nucleus (not shown). A few hours after loss of CycA2-eYFP in the cytoplasm, CycA2-eYFP signal disappeared also from the nucleus (Fig. 3A). The loss of cytoplasmic CycA2-eYFP occurred at similar time-scales after DNA damage as what we and others previously described for p53 and p21-dependent nuclear translocation of CycB1-eYFP (Krenning et al., 2014; Mullers et al., 2014). We therefore wondered if p21 or p53 play a role in the regulation of CycA2 localisation after DNA damage. To this end, we transfected cells with either p21 or p53 siRNAs for 48 h and assessed the dynamics of CycA2-eYFP upon DNA damage. Interestingly, p21 and p53 knockdown impaired both the cytoplasmic and subsequent nuclear loss of CycA2-eYFP, p53 knockdown being the most evident with less than 40 % of cells losing cytoplasmic CycA2 (Fig. 3B, left). Similarly, cells expressing only nuclear CycA2-eYFP at the time-point of addition of Etoposide retained nuclear CycA2-eYFP after p21 or p53 knockdown (Fig. 3B, right).

Altogether, these results suggest that p21 and p53 regulate CycA2 localisation and protein levels upon DNA damage.

p21 can modulate CycA2 localisation to the cytoplasm

Given the indications of p21 and p53 playing a role in CycA2 localisation upon DNA damage, we decided to further explore their contribution to CycA2 regulation in unperturbed conditions. To do so we used CRISPR/Cas9 to establish p21 or p53 deficient RPE cell lines (Fig. S3A). We imaged p21$^{-/-}$, p53$^{-/-}$, and WT RPE cells and recorded the cumulative mitotic entry of each cell line. The three cell-lines entered mitosis at a similar rate, indicating that these cell lines show no major differences in proliferation (Fig. S3B). Next, we fixed cells after a short pulse with EdU, stained using DAPI and antibodies against CycA2, and quantified the levels of nuclear and cytoplasmic CycA2 in S or G2 phase (Fig. 4A). We observed that both p21$^{-/-}$ and p53$^{-/-}$ cell lines accumulated nuclear CycA2 similar to the WT cell line (Fig. 4B). However, quantification of cytoplasmic CycA2 revealed that p21 deficiency led to an increase in cytoplasmic CycA2 in both S and G2 phase (Fig. 4B). To a lower extent, we also detect increased cytoplasmic CycA2 staining in p53$^{-/-}$ G2 cells. Finally, we immunoprecipitated CycA2 YFP from cells synchronized in G2 and found that it specifically interacted with p21 in both cytosolic and nuclear fractions (Fig. 2E). Combined, our results indicate that p21 negatively regulates cytoplasmic localisation of CycA2 both in the presence and absence of externally induced DNA damage.

CycA2 triggers Plk1 activation at the S/G2 transition

The cytoplasmic appearance of CycA2 at the S/G2 transition coincides with activation of Plk1 and Cdk1, raising the possibility that these events are linked (Akopyan et al., 2014). We find that Cdk1 or Plk1 inhibition does not impede CycA2 appearance in cytoplasm, suggesting that CycA2 localisation change is not downstream of mitotic kinase activation (Fig. 2A). To test whether CycA2 is required for Plk1 activation, we depleted CycA2 by siRNA and monitored S-phase progression by a PCNA chromobody and Plk1 activation by a FRET-based biosensor (Akopyan et al., 2014). Whereas control cells show Plk1 activation as PCNA foci sharply decrease at the S/G2 border, CycA2 depleted cells showed no sharp decrease in PCNA foci. Rather, the amount and intensity of PCNA foci gradually decreased, and Plk1 activity remained low (Fig. 5A, B). This shows that Plk1 activation is impaired after CycA2 depletion, but also suggests that the S/G2 transition is impaired in the absence of CycA2. To assess whether Cyclin-Cdk complexes affected Plk1 activity after completion of the S/G2 transition, we next added inhibitors to Cdk1 and Cdk2 to G2 cells. We find that addition of either Cdk1 or Cdk2 inhibitor disturbed Plk1 activity as well as the pT210 modification of PLK1, showing the most prominent effect with a combination of both inhibitors (Fig. 5C, 5D). Thus, both CycA2 RNAi and addition of Cdk inhibitor impairs Plk1 activation, suggesting that CycA2 stimulates Plk1 activation.

We and others previously showed that Plk1 is activated by Aurora A, in a reaction that requires the cofactor Bora (Macurek et al., 2008; Seki et al., 2008). In addition, Bora is heavily phosphorylated by CycB1-Cdk1 at mitotic entry, and the integrity of these phosphorylation sites is important for Plk1 activation (Parrilla et al., 2016; Tavernier et al., 2015; Thomas et al., 2016). Here we find that the Aurora A-mediated phosphorylation of Plk1 was further stimulated by CycA2-Cdk2 activity in the presence of Bora, suggesting that similarly as CycB1-Cdk1, also CycA2-Cdk2 can stimulate activation of Plk1 (Figure 5E) (Gheghiani et al., 2017). To assess if and where CycA2 forms a complex with Plk1 and Bora, we immunoprecipitated CycA2 from nuclear or cytoplasmic extracts of G2 cells and probed for interactors. Cdk1 and Cdk2 co-immunoprecipitated with CycA2 from both nuclear and cytoplasmic extracts, suggesting that CycA2-Cdk1 and CycA2-Cdk2 are present throughout the cell (Figure 2E). Interestingly however, we found that both Bora and Plk1 co-immunoprecipitated with CycA2 specifically in the cytoplasm (Figure 5F). Thus, although Plk1 is active in both nucleus and cytoplasm and Plk1 is in close proximity to CycA2 in both compartments (Figure S4), the activating interaction involving Bora occurs in the cytoplasm. Taken together, our results suggest that cytoplasmic CycA2 plays a key role in activating Plk1.

Discussion

Here we show that CycA2 appears in the cytoplasm at the S/G2 transition. We find that cytoplasmic localization of CycA2 depends on at least two principal components. First, we find that association with Cdk1 stimulates cytoplasmic appearance of CycA2. Second, we find that p21 restricts cytoplasmic CycA2. Both these components are likely complemented by additional mechanisms, as we detect cytoplasmic CycA2 in complex with Cdk2 and p21-negative cells with limited amounts of cytoplasmic CycA2. Although p21 expression occurs independently of p53 in the absence of induced DNA damage, p21 levels in S phase are generally low due to DNA-replication dependent degradation (Kim et al., 2008; Macleod et al., 1995; Nishitani et al., 2008). It therefore remains a possibility that p21, rather than keeping CycA2 nuclear during an unperturbed S-phase, functions as a safety mechanism that restricts cytoplasmic appearance of CycA2 in case of premature positive stimulus.

The regulated appearance of CycA2 in the cytoplasm at the S/G2 transition suggests that CycA2 can direct Cdk activity both in a temporal and spatial manner. This is similar to CycB1, whose change in localisation just prior to mitosis provides access to nuclear substrates (Pines and Hunter, 1991). We identify Bora as a substrate for CycA2 in the cytoplasm, indicating that CycA2 appearance in cytoplasm links to activation of Plk1. Given that multiple cytoplasmic targets of CycA2 have been described, and that Cdk2 is identified as a major interaction hub in the cytoskeleton, we note the possibility that other processes are differentially regulated before and after completion of S-phase (Arsic et al., 2012; Bendris et al., 2014; Kanakkanthara et al., 2016; Thul et al., 2017; Tsang et al., 2007; Woodman et al., 1993).

A long standing idea in the cell cycle field has been that upon stress, cell cycle progression can be delayed by altering the localisation of key proteins as Cdc25B, Cdc25C, and Cyclin B1 (Takizawa and Morgan, 2000). Recently, we and others showed that upon DNA damage, terminal cell cycle exit from G2 phase is marked by a p21-dependent abrupt translocation of Cyclin B1 to the nucleus (Krenning et al., 2014; Mullers et al., 2014). Here we found that after DNA damage, CycA2 localised to the nucleus. Similarly to CycB1, the DNA-damage dependent nuclear localisation of CycA2 depended on p53 and p21 (Krenning et al., 2014; Mullers et al., 2014). Interestingly, early after DNA damage a low level of Cdk activity is sustained and Bora remains associated with Plk1 (Bruinsma et al., 2017; Mullers et al., 2017). This opens up the possibility that CycA2-dependent cytoplasmic functions can be retained early during a DDR.

The S/G2 transition is marked by an increase in Cdk1 and Plk1 activities, which through feedback loops slowly build up until enforcing mitotic entry (Akopyan et al., 2014). Whereas Plk1 increases Cdk1 activity by phosphorylation of Wee1 and Cdc25, Plk1 activation requires Cdk-dependent phosphorylation of the Plk1 interactor Bora (Parrilla et al., 2016; Tavernier et al., 2015; Thomas et al., 2016). How to separate the hen from the egg and identify a starting point in these feedback loops has remained an unsolved question, but several studies have suggested a role for CycA2 as an initiating activity (De Boer et al., 2008; Fung et al., 2007; Gheghiani et al., 2017; Gong et al., 2007; Mitra and Enders, 2004). However, CycA2-Cdk2 activity is present during S-phase, raising the question why Plk1 activation is detected at the S/G2 transition (Akopyan et al., 2014; Spencer et al., 2013). Interestingly, whereas proteins as Plk1 and CycB1-Cdk1 are both nuclear and cytoplasmic, Bora appears exclusively cytoplasmic (Bruinsma et al., 2015; Feine et al., 2014).

We propose a model in which the rising cytoplasmic activity of CycA2-Cdk initiates activation of Plk1 through phosphorylation of the cytoplasmic cofactor Bora (Fig. 6). Late in G2, combined activities of CycA2-Cdk and CycB-Cdk1 further increase activation of Plk1 through massive modification of Bora, eventually resulting in commitment to mitosis and protection of Bora from SCF-dependent degradation (Feine et al., 2014; Gheghiani et al., 2017; Tavernier et al., 2015; Thomas et al., 2016). We find no evidence that Cdk1 or Plk1 activities influence CycA2 localisation, supporting the idea that rather than a component of feedback loops, CycA2 appearance in the cytoplasm functions as a trigger for mitotic kinase activation.

Acknowledgements

We thank the members of Lindqvist and Macurek labs for comments and suggestions. This work was supported by grants from the Swedish Research Council, the Swedish Foundation for Strategic Research, the Swedish Cancer Society and the Grant Agency of the Czech Republic (17-04742S).

Materials and Methods

Cell culture

Human hTERT-RPE1 (hereafter referred to as RPE), U2OS and HeLa cells were cultured in an ambient-controlled incubator at 37°C and 5% CO_2. All cells were a kind gift from René Medema and were regularly controlled for mycoplasma infection. RPE cells were cultured using DMEM-F12 + GlutaMAX (Invitrogen) supplemented with 10% heat-inactivated FBS (HyClone) and 1% P/S (HyClone). U2OS and HeLa cells were cultured using DMEM + GlutaMAX (Invitrogen) supplemented with 6% heat-inactivated fetal bovine serum (FBS, HyClone) and 1% Penicillin/Streptomycin (P/S, HyClone). For adeno-associated virus production, HEK293 cells were cultured using DMEM + GlutaMAX (Invitrogen) supplemented with 10% heat-inactivated fetal bovine serum (FBS, HyClone) and 1% Penicillin/Streptomycin (P/S, HyClone). For live-cell imaging experiments the medium of the cells was changed to Leibowitz-15 (Invitrogen) supplemented with 10% FBS (HyClone) and 1% P/S (HyClone) at least 12h before initiation of the imaging.

Establishment of cell lines

RPE CycA2-eYFP cells were obtained by adeno-associated (AAV)-mediated homologous recombination as previously described (Akopyan et al., 2014). Briefly, the targeting cassette was designed to contain an arm of 1.1 kb of homology with the sequence directly 5' of the *CCNA2* Stop codon followed by the ORF of EYFP and another arm of homology 1.016 kb with the 3' UTR of the *CCNA2* gene. Adeno-associated viruses containing the homology cassette were produced and used to transduce RPE cells. Four days after transduction cells were sorted by FACS to enrich the YFP-positive population. After two rounds of sorting, single YFP positive cells were seeded in 96-well plates and clones which were validated by Western blot and live-cell imaging. Knock out of *TP53* and *p21* in RPE cells using CRISPR/Cas9 was generated as described previously (Pechackova et al., 2016) and independent clones were validated by western blotting and sequencing of the genetic loci.

Cell synchronization

RPE or RPE CycA2-eYFP cells were synchronized in G0 by growing to confluency, split to fresh medium supplemented with thymidine (2 mM) and grown for 40 h. Cells were released to fresh medium and collected after 5h. Synchronization efficiency was validated by flow cytometry using 4n DNA content and absence of pS10-H3 staining as G2 markers. Typically, this protocol yielded >95% G2 population and less than 0.5 % mitotic cells.

Cell fractionation and Immunoprecipitation

Cells were fractionated using hypotonic lysis as previously described (Andersen et al., 2002). Briefly, cells were collected by trypsinization and centrifugation (300 *g* for 5 min at 4°C), and washed with PBS. The cell pellet was resuspended in 5× packed cell volume of hypotonic buffer A (10 mM Hepes-KOH, pH 7.9, 10 mM KCl, 1.5 mM $MgCl_2$, 0.5 mM DTT, and 0.5 mM PMSF) supplemented with a cocktail of protease inhibitors (cOmplete, EDTA free; Roche) and phosphatase inhibitors (PhosSTOP, Roche) and incubated on ice for 5 min. Next, the cells were spun down at 500 *g* for 5 min, suspended in 2× packed cell volume of supplemented buffer A and dounced using a tight-fitting pestle. Nuclei were collected by centrifugation at 500 *g* for 5 min at 4°C. Supernatant was centrifuged 20000g 10 min 4°C, supplemented with NaCl and Triton X-100 to 150 mM and 0.1 % final concentration, respectively and used as cytoplasmic fraction. Nuclei were cleaned by centrifugation over sucrose gradient, lysed in lysis buffer (10 mM HEPES pH 7.9, 10 mM KCl, 150 mM NaCl, 1.5 mM MgCl2, 0.1 % NP-40, 0.5mM DTT, 0.5 mM PMSF supplemented with protease inhibitor cocktail and PhosSTOP), sonicated and cleared by centrifugation at 20000 g 10min 4°C. For IP 2 mg of cytoplasmic and nuclear extracts were incubated with either 15 ml GFP Trap beads (Chromotek) for 1 h at 4°C or 1-1.5 μg IgG overnight at 4°C, Protein A/G Ultralink beads were added for last 2 h. Beads were washed four times with lysis buffer and precipitates were eluted to SDS-PAGE sample buffer.

Inhibitors

For live-cell imaging and quantitative immunofluorescence experiments, the following inhibitors were used at the indicated concentrations for 4 h unless indicated differently in the experiments: RO-3306 at 10 μM (Cdk1 inhibitor; Calbiochem), NU6140 at 10 μM (Cdk2 inhibitor; Calbiochem), Roscovitine at 25 μM (broad Cdk inhibitor; Selleck Chemicals), MK-1775 at 100 μM (Wee1 inhibitor; Selleck Chemicals), BI2536 at 100 nM (Plk1 inhibitor, Selleck Chemicals), MLN8237 at 100nM (Aurora A inhibitor; Selleckchem), Etoposide 2μM (topoisomerase II inhibitor; Sigma Aldrich), Neocarzinostatin at 2 nM (toxin; Sigma Aldrich), KU60019 at 10 μM (ATM inhibitor; Tocris Bioscience), VE821 at 10 μM (ATR inhibitor; Selleckchem), Cycloheximide at 10 μg/ml (inhibitor of protein synthesis; Sigma Aldrich), Thymidine at 2.5 mM (Sigma Aldrich) and Hydroxyurea at 2 mM (ribonucleotide reductase inhibitor; Sigma Aldrich).

siRNA transfection

SMARTpool ON-TARGET plus siRNAs targeting CycA2, Cdk1, Cdk2, p21 or p53 as well as a scrambled control siRNA were purchased from Dharmacon and employed at a concentration of 20nM using HiPerFect transfection reagent (Qiagen) and OptiMEM (Invitrogen) at 48h and 24h before live-cell imaging or fixation.

Live-cell microscopy

For live cell imaging experiments, 10.000 cells were seeded in 96-well imaging plates (BD Falcon) using Leibowitz-15 medium (Invitrogen) 16 h prior to initiation of the imaging on an ImageXpress system (Molecular Devices) using a 20x NA 0.45 objective. Images were processed and analysed using ImageJ. Nuclei and cytoplasms were selected by manual drawing. Integrated intensities were calculated for nuclei whereas an area of the cytoplasm was measured and mean or median intensities were measured for cytoplasmic quantifications. FRET microscopy was performed as in (Hukasova et al., 2012) and simultaneous monitoring of FRET and a PCNA chromobody was performed as in (Akopyan et al., 2014).

Antibodies

The following antibodies were: GFP (1:400; ab13970 abcam), Cyc A2 (1:100 #sc-751, Santa Cruz), CycA2 (1:500; #4656 Cell Signalling), Plk1 (ab14210; Abcam), affinity purified mouse anti pT210-Plk1 (clone K50-483, Becton Dickinson), affinity purified rabbit anti-Bora (Bruinsma et al., JCS 2014), Cdk1 (sc-54, Santa Cruz and #9116 Cell Signalling), Cdk2 (sc-163, Santa Cruz and #2564 Cell Signalling), GAPDH (1:5000; G9545 Sigma Aldrich), H2B (1:1000; ab1790 abcam), β-Tubulin (1:500, #2128S Cell Signalling), Alexa Fluor 488-Goat anti-chicken (1:1000; #A11039 Life Technologies) and Alexa Fluor 647-Donkey anti-rabbit (1:1000; #A31537 Life Technologies).

Quantitative immunofluorescence

For quantitative immunofluorescence experiments 10.000 cells were seeded 16h before the different treatments with inhibitors. For siRNA transfections, 5.000 cells were seeded instead. Twenty minutes before fixation EdU (5-ethynyl-2’-deoxyuridine, Molecular probes) was added in all the experiments. Cells were fixed using 3.7% formaldehyde (Sigma Aldrich) for 5 minutes and permeabilised using -20°C methanol (Sigma Aldrich) for 2 minutes, blocking was performed using 2% bovine albumin serum (BSA; Sigma Aldrich) in TBS supplemented with 0.1% Tween20 (TBS-T). After blocking, cells were incubated with primary antibodies at 4°C overnight. After washing, cells were incubated with secondary antibodies and DAPI for 1h at room temperature. Click chemistry was performed after wash of the secondary antibody using a mixture of 100mM Tris, 1mM $CuSO_4$, 100mM ascorbic acid and fluorescent dye (#A10277 and #A10266, Invitrogen) and incubated for 1h at room temperature. Images were acquired on an ImageXpress system (Molecular Devices) using either a 20x (NA) objective or a 40x NA 0.6 objective. Images were manually screened for wrong cells and processed and analysed using CellProfiler (Carpenter et al., 2006) to identify and measure nuclear and cytoplasmic fluorescence intensity of single cells. Cell cycle stages were determined setting a threshold both on DAPI and EdU levels.

In vitro kinase assay

Kinase dead Plk1-K82R, GST-Bora and GST-Aurora-A were purified from bacteria as described (Macurek et al., 2008) and incubated with CycA2/Cdk2 (100 ng/reaction, Biaffin GmbH) in a kinase buffer (25 mM MOPS pH 7.2, 12.5 mM glycerol 2-phosphate, 25 mM MgCl2, 5 mM EGTA, 2 mM EDTA and 0.25 mM DTT) supplemented with 100 µM ATP and 5 µCi 32P-γ-ATP at 30°C for 30 min. After separation of proteins by SDS-PAGE, phosphorylation was detected by autoradiography or by pT210-Plk1 antibody.

Proximity ligation assay (PLA)

RPE CycA2-eYFP cells were fixed for 10 min with 4 % paraformaldehyde in PBS and permeabilized with 0.2 % Triton X-100 for 5 min at room temperature. Proximity ligation assay (PLA) was performed using mouse anti-PLK1, rabbit anti-cyclin A antibodies and Duolink reagent according to the manufacturers protocol (Sigma-Aldrich). YFP signal was used to identify cells with cytoplasmic CycA2. Signal was imaged by a Leica SP5 confocal microscope using 63 X oil objective.

Figure legends

Figure 1. Cyclin A2 accumulates in the cytoplasm at the S/G2 transition

(**a**) Time-lapse imaging through mitosis of a single RPE cell gene-targeted to express CycA2-eYFP. Time between images is 20 minutes.

(**b**) Quantification of CycA2-eYFP mean intensity in the nucleus (left) and mean intensity in the cytoplasm (middle) of 20 individual cells over time. Cells were synchronised *in silico* to set t=0 at mitosis. The black dotted line represents the average fluorescence intensity of all the cells measured. Plot of the average of nuclear and cytoplasmic mean intensity of 20 cells (right).

(**c**) RPE CycA2-eYFP cells were incubated for 20 min with EdU and fixed. Left graphs shows quantification of nuclear and cytoplasmic integrated intensity of GFP staining versus nuclear DAPI intensity in at least 1500 cells; each dot represents one cell. Middle graph shows nuclear versus cytoplasmic integrated intensities of GFP staining; the grey square indicates the gating for expressors of both nuclear and cytoplasmic CycA2-eYFP. Right graphs show integrated EdU intensity versus integrated DAPI intensity, with or without gating for expressors of both nuclear and cytoplasmic CycA2-eYFP (bottom right).

(**d**) RPE cells were treated as in (c), with the difference that at least 1200 cells were quantified and GFP antibody was replaced by CycA2 antibody.

(**e**) Western blot of nuclear and cytoplasmic fractions of unsynchronised RPE-CycA2-eYFP cells using the indicated antibodies.

(**f**) Quantification of the percentage of cells accumulating CycA2-eYFP in the cytoplasm after different treatments. Cells were treated with DMSO (Control), Thymidine (THY) or Hydroxyurea (HU) and imaged. The number of cells accumulating CycA2 in the cytoplasm was recorded and plotted as a percentage of the total number of cells tracked.

All experiments were repeated at least three times.

Figure 2. Cdk1 can contribute to cytoplasmic accumulation of Cyclin A2

(**a**) Western blot of cells transfected with Cdk1, Cdk2 or scrambled (Control) siRNAs for 48 h. Samples were prepared from 4 wells in a 96-well plate to mimic conditions used for microscopy.

(b) Amount of cells going through mitosis during 16 h after knock down of Cdk1 or Cdk2 for 48 h (left). Duration of mitosis in the indicated knockdown conditions (right).

(c) Cells were transfected with siRNAs for either Cdk1 or Cdk2 for 48 h, incubated with EdU for 20 min and fixed. Arrows indicate G2 cells with low cytoplasmic CycA.

(**d**) Quantification of cytoplasmic and nuclear integrated intensities of CycA2 in at least 500 RPE cells imaged as in (c). Cells were gated for DAPI and EdU levels and assigned to S phase (green dots) or G2 phase (red dots). Each dot represents one cell; the percentages indicate the proportion of S and G2 phase cells in each condition. Numbers to right show amount of cells within indicated gate and total amount of G2 cells.

(**e**) RPE CycA2 YFP or RPE cells were synchronized in G2, separated to cytosolic and nuclear fractions and immunoprecipitated with GFP Trap (left) or with control IgG and CycA2 antibody (right). Proteins bound to the carrier were probed with indicated antibodies.

A and b were repeated twice, the remaining experiments were repeated at list three times.

Figure 3. DNA damage and the DNA damage response can modulate cytoplasmic accumulation of Cyclin A2-eYFP

(**a**) Time-lapse images of RPE CycA2-eYFP cell treated with Etoposide (arrow). Time between images is 20 minutes.

(**b**) Quantification of the dynamics of cytoplasmic and nuclear CycA2-eYFP after DNA damage. RPE CycA2-eYFP cells were transfected with p21, p53 or control siRNAs for 48 h and treated with Etoposide at t=0. Single cells were tracked over time and the time point of cytoplasmic loss of CycA2-eYFP were recorded. Left graphs show at least 100 cells that contained cytoplasmic CycA2-eYFP at time point of addition of Etoposide. Right graphs show at least 90 cells that contained only nuclear CycA2-eYFP at time point of addition of Etoposide.

All experiments were repeated at least three times.

Figure 4. p21 can modulate CycA2 localisation to the cytoplasm

(**a**) WT, p21-/- or p53-/- RPE cells were incubated for 20 min with EdU and fixed. Graph shows quantification of integrated intensity of EdU staining versus nuclear DAPI intensity in at least 1500 cells; each circle represents one cell. The large grey rectangle indicates EdU positive cells and the small grey rectangle indicates EdU-negative 4N cells used for quantification in b.

(**b**) Quantification of nuclear and cytoplasmic integrated intensity of CycA2 in WT, $p53^{-/-}$ and $p21^{-/-}$ RPE cells in S-phase (top) and in G2 phase (bottom), gated as shown in a. Box plots indicate 90, 75, 50, 25, and 10 percentiles. Squares indicate average value. *** indicates p<0.00005, students t-test.

All experiments were repeated at least three times.

Figure 5. Cytoplasmic CycA2 can activate Plk1

(a) Time-lapse sequence of U2OS cells expressing Plk1 FRET reporter and PCNA chromobody. Time points (h) are indicated in figure. Top Ctrl siRNA, bottom CycA2 siRNA.

(b) Quantification of individual cells, imaged as in (a). Red line shows 1/FRET and blue line shows PCNA foci.

(c) Inhibition of Cdk activity in U2OS cells expressing Plk1 FRET reporter. Cells with intermediate Plk1 FRET signal, indicative of G2 phase, were followed after addition of indicated inhibitors. Graph shows average and s.e.m of at least 10 cells per condition.

(d) Inhibition of Cdk activity in RPE synchronized in G2 decrease the level of Plk1 phosphorylation at T210.

(e) Phosphorylation of Bora by CycA2/Cdk2 promotes modification of Plk1 at T210 mediated by Aurora-A. Empty arrowhead indicates position of the kinase dead Plk1, full arrowhead indicates position of Bora.

(f) Cytosolic and nuclear extracts from RPE cells synchronized in G2 were subjected to immunoprecipitation with anti-CycA2 or anti-Plk1 and bound proteins were probed with indicated antibodies.

All experiments were repeated at least three times.

Figure 6. A model for Plk1 activation by cytoplasmic CycA2.

Cytoplasmic appearance of CycA2 (cA2) at the S/G2 transition enables phosphorylation of Bora (B). Phosphorylated Bora interacts with Plk1 and stimulates Aurora A (Aur A)–mediated phosphorylation of Plk1 T210. This is amplified by consequent CycB1 (cB1)-mediated phosphorylation of Bora.

Supplementary figure 1. Characterization of CycA2-eYFP cells

(**a**) Western blot of RPE and RPE CycA2-eYFP cell lines, incubated with the indicated antibodies. Cells were treated with CycA2 siRNA for 24 h, STLC for 16 h, or Etoposide for 24 h.

(**b**) Time-lapse imaging of a single U2OS-CycA2-eYFP cell growing on a fibronectin-coated micropattern. Images were acquired every 20 minutes.

Supplementary figure 2. Cyclin A2-eYFP cytoplasmic appearance after modulation of Cdk activity

(**a**) Quantification of nuclear (left) and cytoplasmic (right) accumulation of CycA2-eYFP in at least 17 single cells treated with DMSO (top), RO-3306 (middle) or Nu6140 (bottom) for 4 hours; each track represents a single cell. Cells were selected based on clear but low cytoplasmic CycA2-eYFP signal at time point of inhibitor addition, and synchronised *in silico* at the time point when cells reached a threshold of cytoplasmic CycA2-eYFP (indicated with the grey dotted line). (Below) Average of nuclear (top lines) and cytoplasmic (bottom lines) intensities. Error bars show SD.

(**b**) Quantification of at least 95 single RPE-CycA2-eYFP cells upon treatment with either DMSO (control) or Wee1 inhibitor (MK1775). Cells were treated with the drugs and tracked using live-cell imaging. Each track represents one single cell, the black dot represents the first time point when cytoplasmic CycA2 can be detected and the red dot indicates mitotic entry. Overlap of the cumulative appearance of cytoplasmic CycA2 in the two different treatments (right).

Supplementary figure 3. Characterization of p53 and p21 knockout cells

(**a**) Parental RPE, RPE-TP53-KO and RPE-p21-KO cells were treated with etoposide for 6 h and whole cell lysates were probed with indicted antibodies. Two independent clones were probed for each knock-out cell line.

(**b**) Cumulative mitotic entry of at least 280 RPE, RPE p53$^{-/-}$, and RPE p21$^{-/-}$ cells.

Supplementary figure 4. Proximity ligation between Cyclin A2 and Plk1

RPE CycA2-eYFP cells were fixed and probed for Proximity ligation assay using mouse anti-Plk1 and rabbit-anti-CycA2 antibodies. Representative image of a cell with strong cytoplasmic presence of CycA2-eYFP is shown. Neighbouring cell with minimal CycA2-eYFP expression indicates background signal.

References

Akopyan, K., Silva Cascales, H., Hukasova, E., Saurin, A.T., Mullers, E., Jaiswal, H., Hollman, D.A., Kops, G.J., Medema, R.H., and Lindqvist, A. (2014). Assessing kinetics from fixed cells reveals activation of the mitotic entry network at the S/G2 transition. Mol Cell *53*, 843-853.

Andersen, J.S., Lyon, C.E., Fox, A.H., Leung, A.K., Lam, Y.W., Steen, H., Mann, M., and Lamond, A.I. (2002). Directed proteomic analysis of the human nucleolus. Curr Biol *12*, 1-11.

Arsic, N., Bendris, N., Peter, M., Begon-Pescia, C., Rebouissou, C., Gadea, G., Bouquier, N., Bibeau, F., Lemmers, B., and Blanchard, J.M. (2012). A novel function for Cyclin A2: control of cell invasion via RhoA signaling. J Cell Biol *196*, 147-162.

Bendris, N., Cheung, C.T., Leong, H.S., Lewis, J.D., Chambers, A.F., Blanchard, J.M., and Lemmers, B. (2014). Cyclin A2, a novel regulator of EMT. Cell Mol Life Sci *71*, 4881-4894.

Bloom, J., and Cross, F.R. (2007). Multiple levels of cyclin specificity in cell-cycle control. Nat Rev Mol Cell Biol *8*, 149-160.

Bruinsma, W., Aprelia, M., Garcia-Santisteban, I., Kool, J., Xu, Y.J., and Medema, R.H. (2017). Inhibition of Polo-like kinase 1 during the DNA damage response is mediated through loss of Aurora A recruitment by Bora. Oncogene *36*, 1840-1848.

Bruinsma, W., Aprelia, M., Kool, J., Macurek, L., Lindqvist, A., and Medema, R.H. (2015). Spatial Separation of Plk1 Phosphorylation and Activity. Front Oncol *5*, 132.

Cardoso, M.C., Leonhardt, H., and Nadal-Ginard, B. (1993). Reversal of terminal differentiation and control of DNA replication: cyclin A and Cdk2 specifically localize at subnuclear sites of DNA replication. Cell *74*, 979-992.

Carpenter, A.E., Jones, T.R., Lamprecht, M.R., Clarke, C., Kang, I.H., Friman, O., Guertin, D.A., Chang, J.H., Lindquist, R.A., Moffat, J.*, et al.* (2006). CellProfiler: image analysis software for identifying and quantifying cell phenotypes. Genome Biol *7*, R100.

De Boer, L., Oakes, V., Beamish, H., Giles, N., Stevens, F., Somodevilla-Torres, M., Desouza, C., and Gabrielli, B. (2008). Cyclin A/cdk2 coordinates centrosomal and nuclear mitotic events. Oncogene *27*, 4261-4268.

Feine, O., Hukasova, E., Bruinsma, W., Freire, R., Fainsod, A., Gannon, J., Mahbubani, H.M., Lindqvist, A., and Brandeis, M. (2014). Phosphorylation-mediated stabilization of Bora in mitosis coordinates Plx1/Plk1 and Cdk1 oscillations. Cell Cycle *13*, 1727-1736.

Frouin, I., Toueille, M., Ferrari, E., Shevelev, I., and Hubscher, U. (2005). Phosphorylation of human DNA polymerase lambda by the cyclin-dependent kinase Cdk2/cyclin A complex is modulated by its association with proliferating cell nuclear antigen. Nucleic Acids Res *33*, 5354-5361.

Fung, T.K., Ma, H.T., and Poon, R.Y. (2007). Specialized roles of the two mitotic cyclins in somatic cells: cyclin A as an activator of M phase-promoting factor. Mol Biol Cell *18*, 1861-1873.

Furuno, N., den Elzen, N., and Pines, J. (1999). Human cyclin A is required for mitosis until mid prophase. J Cell Biol *147*, 295-306.

Gheghiani, L., Loew, D., Lombard, B., Mansfeld, J., and Gavet, O. (2017). PLK1 Activation in Late G2 Sets Up Commitment to Mitosis. Cell Rep *19*, 2060-2073.

Gong, D., and Ferrell, J.E., Jr. (2010). The roles of cyclin A2, B1, and B2 in early and late mitotic events. Mol Biol Cell *21*, 3149-3161.

Gong, D., Pomerening, J.R., Myers, J.W., Gustavsson, C., Jones, J.T., Hahn, A.T., Meyer, T., and Ferrell, J.E., Jr. (2007). Cyclin A2 regulates nuclear-envelope breakdown and the nuclear accumulation of cyclin B1. Curr Biol *17*, 85-91.

Hein, J.B., and Nilsson, J. (2016). Interphase APC/C-Cdc20 inhibition by cyclin A2-Cdk2 ensures efficient mitotic entry. Nat Commun *7*, 10975.

Hukasova, E., Silva Cascales, H., Kumar, S.R., and Lindqvist, A. (2012). Monitoring kinase and phosphatase activities through the cell cycle by ratiometric FRET. J Vis Exp, e3410.

Jackman, M., Kubota, Y., den Elzen, N., Hagting, A., and Pines, J. (2002). Cyclin A- and cyclin E-Cdk complexes shuttle between the nucleus and the cytoplasm. Mol Biol Cell *13*, 1030-1045.

Kalaszczynska, I., Geng, Y., Iino, T., Mizuno, S., Choi, Y., Kondratiuk, I., Silver, D.P., Wolgemuth, D.J., Akashi, K., and Sicinski, P. (2009). Cyclin A is redundant in fibroblasts but essential in hematopoietic and embryonic stem cells. Cell *138*, 352-365.

Kanakkanthara, A., Jeganathan, K.B., Limzerwala, J.F., Baker, D.J., Hamada, M., Nam, H.J., van Deursen, W.H., Hamada, N., Naylor, R.M., Becker, N.A., *et al.* (2016). Cyclin A2 is an RNA binding protein that controls Mre11 mRNA translation. Science *353*, 1549-1552.

Katsuno, Y., Suzuki, A., Sugimura, K., Okumura, K., Zineldeen, D.H., Shimada, M., Niida, H., Mizuno, T., Hanaoka, F., and Nakanishi, M. (2009). Cyclin A-Cdk1 regulates the origin firing program in mammalian cells. Proc Natl Acad Sci U S A *106*, 3184-3189.

Kim, Y., Starostina, N.G., and Kipreos, E.T. (2008). The CRL4Cdt2 ubiquitin ligase targets the degradation of p21Cip1 to control replication licensing. Genes Dev *22*, 2507-2519.

Krenning, L., Feringa, F.M., Shaltiel, I.A., van den Berg, J., and Medema, R.H. (2014). Transient activation of p53 in G2 phase is sufficient to induce senescence. Mol Cell *55*, 59-72.

Laoukili, J., Alvarez, M., Meijer, L.A., Stahl, M., Mohammed, S., Kleij, L., Heck, A.J., and Medema, R.H. (2008). Activation of FoxM1 during G2 requires cyclin A/Cdk-dependent relief of autorepression by the FoxM1 N-terminal domain. Mol Cell Biol *28*, 3076-3087.

Lindqvist, A., Rodriguez-Bravo, V., and Medema, R.H. (2009). The decision to enter mitosis: feedback and redundancy in the mitotic entry network. J Cell Biol *185*, 193-202.

Liu, D., Matzuk, M.M., Sung, W.K., Guo, Q., Wang, P., and Wolgemuth, D.J. (1998). Cyclin A1 is required for meiosis in the male mouse. Nat Genet *20*, 377-380.

Lukas, C., Sorensen, C.S., Kramer, E., Santoni-Rugiu, E., Lindeneg, C., Peters, J.M., Bartek, J., and Lukas, J. (1999). Accumulation of cyclin B1 requires E2F and cyclin-A-dependent rearrangement of the anaphase-promoting complex. Nature *401*, 815-818.

Macleod, K.F., Sherry, N., Hannon, G., Beach, D., Tokino, T., Kinzler, K., Vogelstein, B., and Jacks, T. (1995). p53-dependent and independent expression of p21 during cell growth, differentiation, and DNA damage. Genes Dev *9*, 935-944.

Macurek, L., Lindqvist, A., Lim, D., Lampson, M.A., Klompmaker, R., Freire, R., Clouin, C., Taylor, S.S., Yaffe, M.B., and Medema, R.H. (2008). Polo-like kinase-1 is activated by aurora A to promote checkpoint recovery. Nature *455*, 119-123.

Maridor, G., Gallant, P., Golsteyn, R., and Nigg, E.A. (1993). Nuclear localization of vertebrate cyclin A correlates with its ability to form complexes with cdk catalytic subunits. J Cell Sci *106 (Pt 2)*, 535-544.

Merrick, K.A., Larochelle, S., Zhang, C., Allen, J.J., Shokat, K.M., and Fisher, R.P. (2008). Distinct activation pathways confer cyclin-binding specificity on Cdk1 and Cdk2 in human cells. Mol Cell *32*, 662-672.

Mitra, J., and Enders, G.H. (2004). Cyclin A/Cdk2 complexes regulate activation of Cdk1 and Cdc25 phosphatases in human cells. Oncogene *23*, 3361-3367.

Moore, J.D., Yang, J., Truant, R., and Kornbluth, S. (1999). Nuclear import of Cdk/cyclin complexes: identification of distinct mechanisms for import of Cdk2/cyclin E and Cdc2/cyclin B1. J Cell Biol *144*, 213-224.

Morgan, D.O. (2007). Cell Cycle: Principles of Control (Oxford University Press).

Mullers, E., Silva Cascales, H., Burdova, K., Macurek, L., and Lindqvist, A. (2017). Residual Cdk1/2 activity after DNA damage promotes senescence. Aging Cell *16*, 575-584.

Mullers, E., Silva Cascales, H., Jaiswal, H., Saurin, A.T., and Lindqvist, A. (2014). Nuclear translocation of Cyclin B1 marks the restriction point for terminal cell cycle exit in G2 phase. Cell Cycle *13*, 2733-2743.

Murphy, M., Stinnakre, M.G., Senamaud-Beaufort, C., Winston, N.J., Sweeney, C., Kubelka, M., Carrington, M., Brechot, C., and Sobczak-Thepot, J. (1997). Delayed early embryonic lethality following disruption of the murine cyclin A2 gene. Nat Genet *15*, 83-86.

Nishitani, H., Shiomi, Y., Iida, H., Michishita, M., Takami, T., and Tsurimoto, T. (2008). CDK inhibitor p21 is degraded by a proliferating cell nuclear antigen-coupled Cul4-DDB1Cdt2 pathway during S phase and after UV irradiation. J Biol Chem *283*, 29045-29052.

Oakes, V., Wang, W., Harrington, B., Lee, W.J., Beamish, H., Chia, K.M., Pinder, A., Goto, H., Inagaki, M., Pavey, S.*, et al.* (2014). Cyclin A/Cdk2 regulates Cdh1 and claspin during late S/G2 phase of the cell cycle. Cell Cycle *13*, 3302-3311.

Pagano, M., Pepperkok, R., Verde, F., Ansorge, W., and Draetta, G. (1992). Cyclin A is required at two points in the human cell cycle. EMBO J *11*, 961-971.

Parrilla, A., Cirillo, L., Thomas, Y., Gotta, M., Pintard, L., and Santamaria, A. (2016). Mitotic entry: The interplay between Cdk1, Plk1 and Bora. Cell Cycle *15*, 3177-3182.

Pechackova, S., Burdova, K., Benada, J., Kleiblova, P., Jenikova, G., and Macurek, L. (2016). Inhibition of WIP1 phosphatase sensitizes breast cancer cells to genotoxic stress and to MDM2 antagonist nutlin-3. Oncotarget *7*, 14458-14475.

Petermann, E., and Caldecott, K.W. (2006). Evidence that the ATR/Chk1 pathway maintains normal replication fork progression during unperturbed S phase. Cell Cycle *5*, 2203-2209.

Petersen, B.O., Lukas, J., Sorensen, C.S., Bartek, J., and Helin, K. (1999). Phosphorylation of mammalian CDC6 by cyclin A/CDK2 regulates its subcellular localization. EMBO J *18*, 396-410.

Pines, J., and Hunter, T. (1991). Human cyclins A and B1 are differentially located in the cell and undergo cell cycle-dependent nuclear transport. J Cell Biol *115*, 1-17.

Pines, J., and Hunter, T. (1994). The differential localization of human cyclins A and B is due to a cytoplasmic retention signal in cyclin B. EMBO J *13*, 3772-3781.

Seki, A., Coppinger, J.A., Jang, C.Y., Yates, J.R., and Fang, G. (2008). Bora and the kinase Aurora a cooperatively activate the kinase Plk1 and control mitotic entry. Science *320*, 1655-1658.

Snapp, E. (2005). Design and use of fluorescent fusion proteins in cell biology.

Spencer, S.L., Cappell, S.D., Tsai, F.C., Overton, K.W., Wang, C.L., and Meyer, T. (2013). The proliferation-quiescence decision is controlled by a bifurcation in CDK2 activity at mitotic exit. Cell *155*, 369-383.

Takizawa, C.G., and Morgan, D.O. (2000). Control of mitosis by changes in the subcellular location of cyclin-B1-Cdk1 and Cdc25C. Curr Opin Cell Biol *12*, 658-665.

Tavernier, N., Noatynska, A., Panbianco, C., Martino, L., Van Hove, L., Schwager, F., Leger, T., Gotta, M., and Pintard, L. (2015). Cdk1 phosphorylates SPAT-1/Bora to trigger PLK-1 activation and drive mitotic entry in C. elegans embryos. J Cell Biol *208*, 661-669.

Thomas, Y., Cirillo, L., Panbianco, C., Martino, L., Tavernier, N., Schwager, F., Van Hove, L., Joly, N., Santamaria, A., Pintard, L.*, et al.* (2016). Cdk1 Phosphorylates SPAT-1/Bora to Promote Plk1 Activation in C. elegans and Human Cells. Cell Rep *15*, 510-518.

Thul, P.J., Akesson, L., Wiking, M., Mahdessian, D., Geladaki, A., Ait Blal, H., Alm, T., Asplund, A., Bjork, L., Breckels, L.M.*, et al.* (2017). A subcellular map of the human proteome. Science *356*.

Tsang, W.Y., Wang, L., Chen, Z., Sanchez, I., and Dynlacht, B.D. (2007). SCAPER, a novel cyclin A-interacting protein that regulates cell cycle progression. J Cell Biol *178*, 621-633.

Woo, R.A., and Poon, R.Y. (2003). Cyclin-dependent kinases and S phase control in mammalian cells. Cell Cycle *2*, 316-324.

Woodman, P.G., Adamczewski, J.P., Hunt, T., and Warren, G. (1993). In vitro fusion of endocytic vesicles is inhibited by cyclin A-cdc2 kinase. Mol Biol Cell *4*, 541-553.

Figure 1. Cyclin A2 accumulates in the cytoplasm at the S/G2 transition

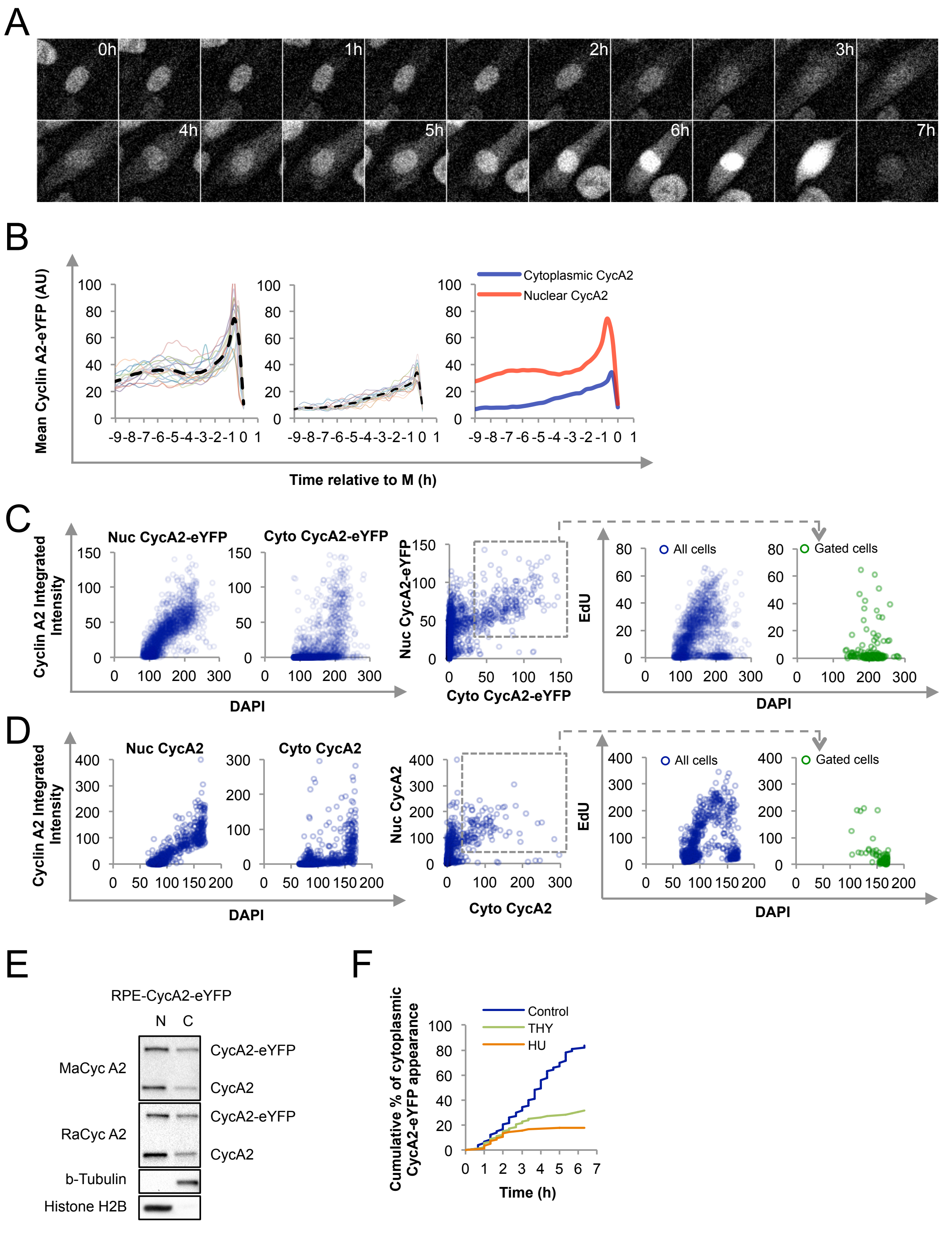

Figure 2. Cdk1 can contribute to cytoplasmic accumulation of Cyclin A2

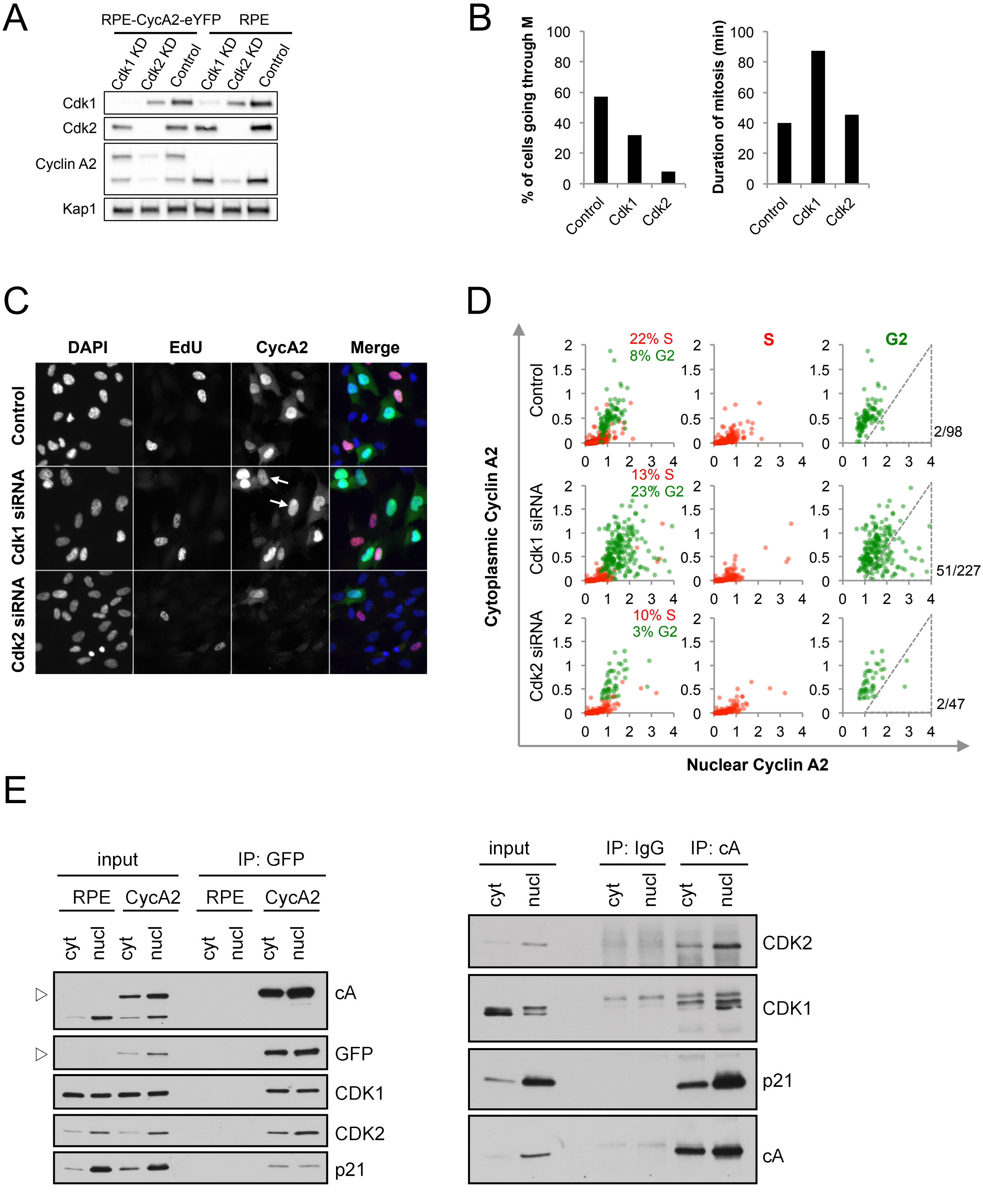

Figure 3. DNA damage and the DNA damage response can modulate cytoplasmic accumulation of Cyclin A2-eYFP

A

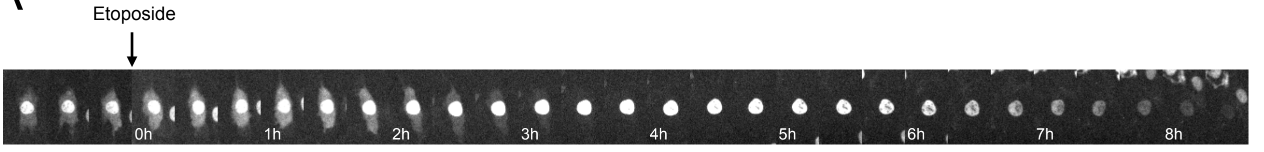

B

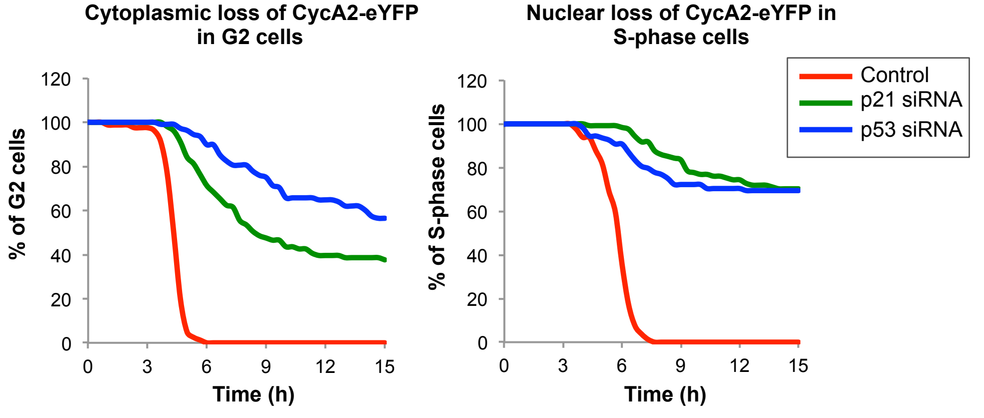

Figure 4. p21 can modulate Cyclin A2 localisation to the cytoplasm

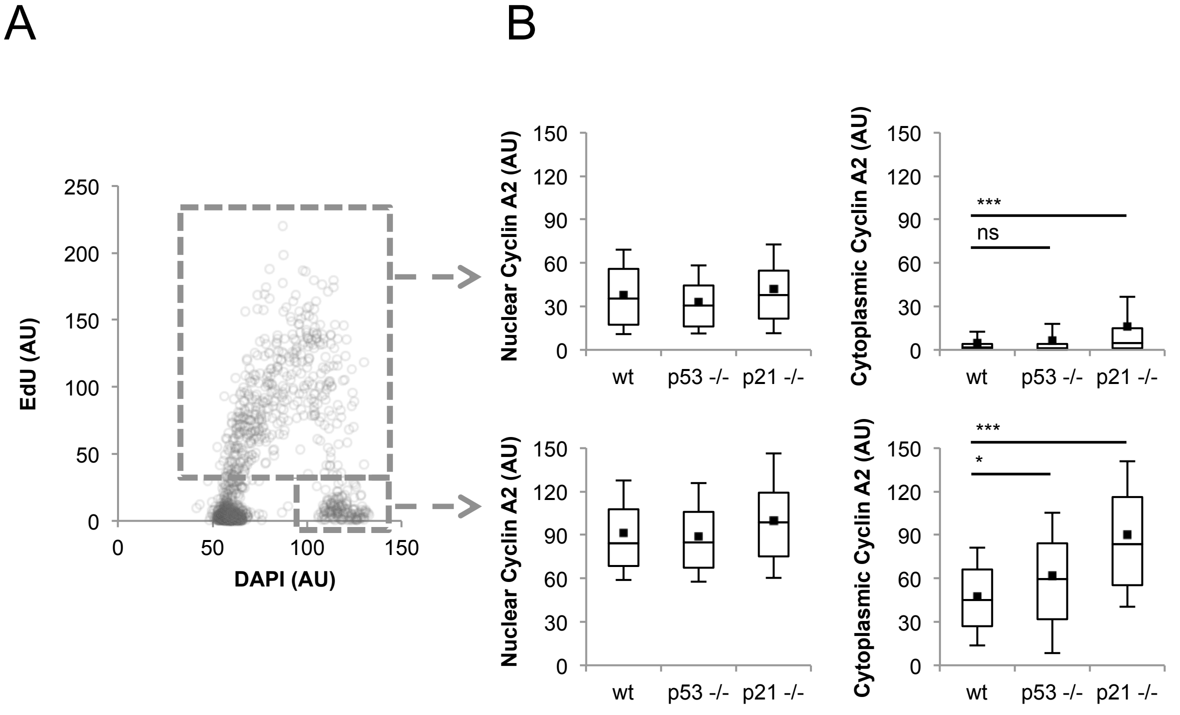

Figure 5. Cytoplasmic Cyclin A2 can activate Plk1

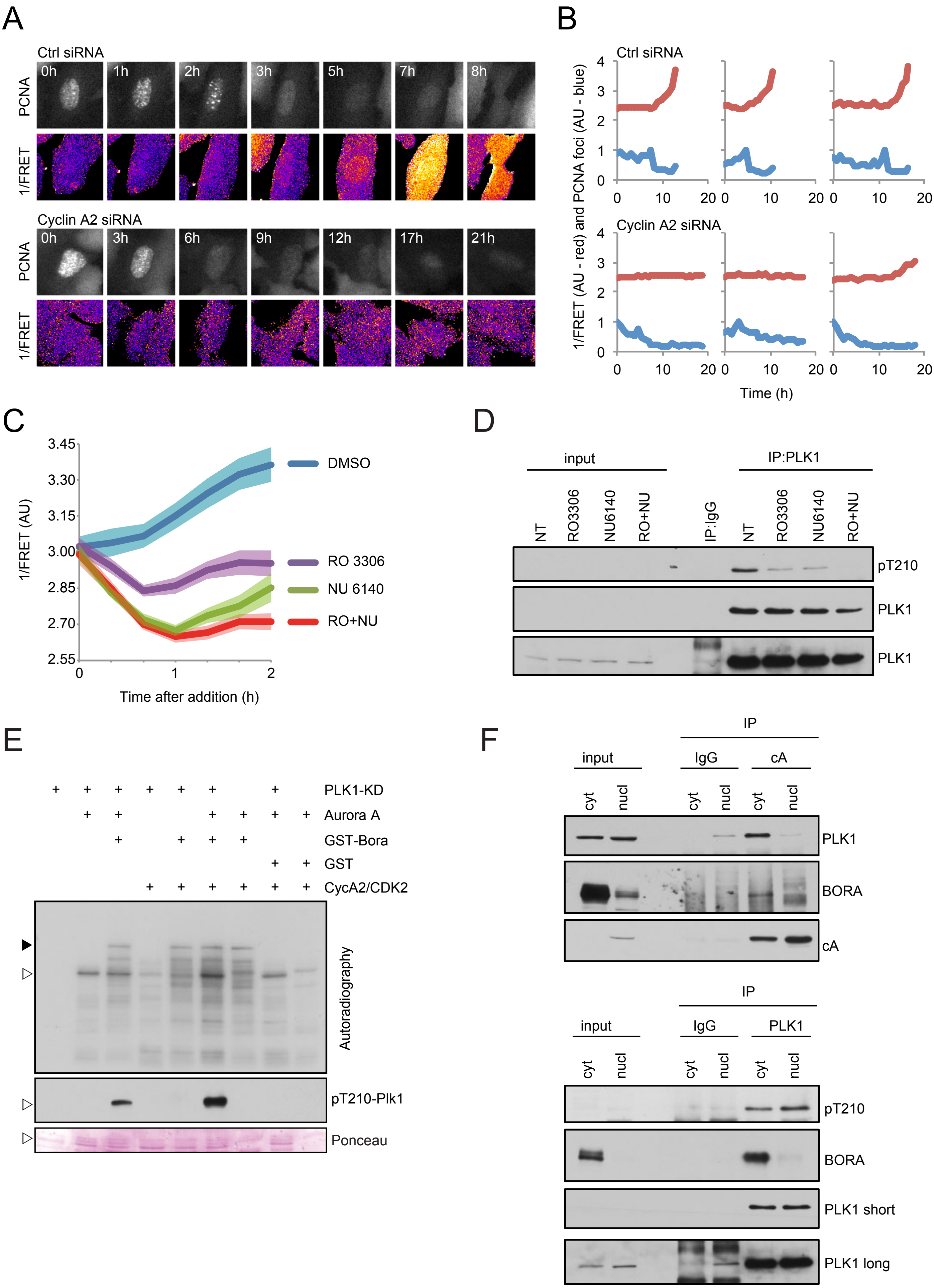

Figure 6. A model for Plk1 activation by cytoplasmic Cyclin A2

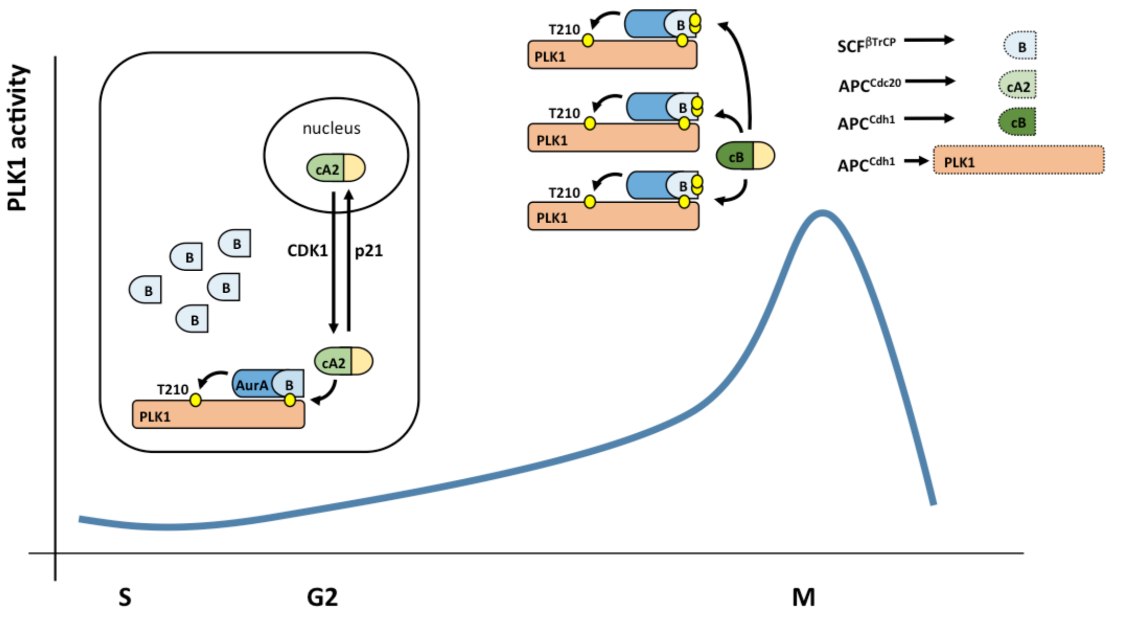

Supplementary Figure 1

A

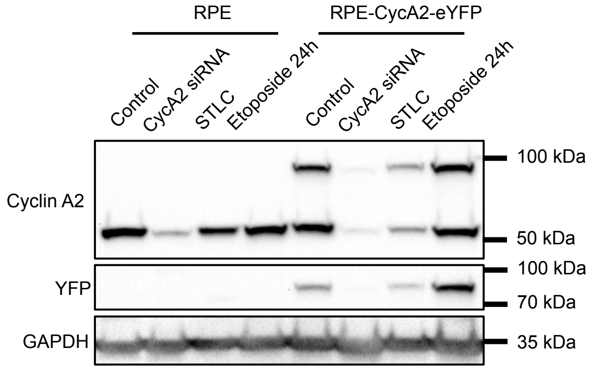

B

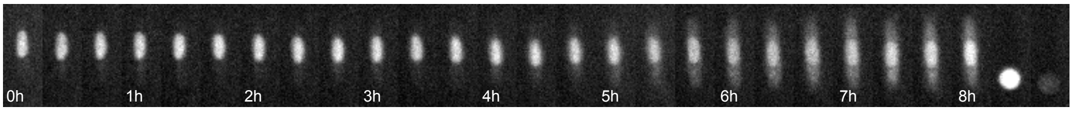

Supplementary Figure 2

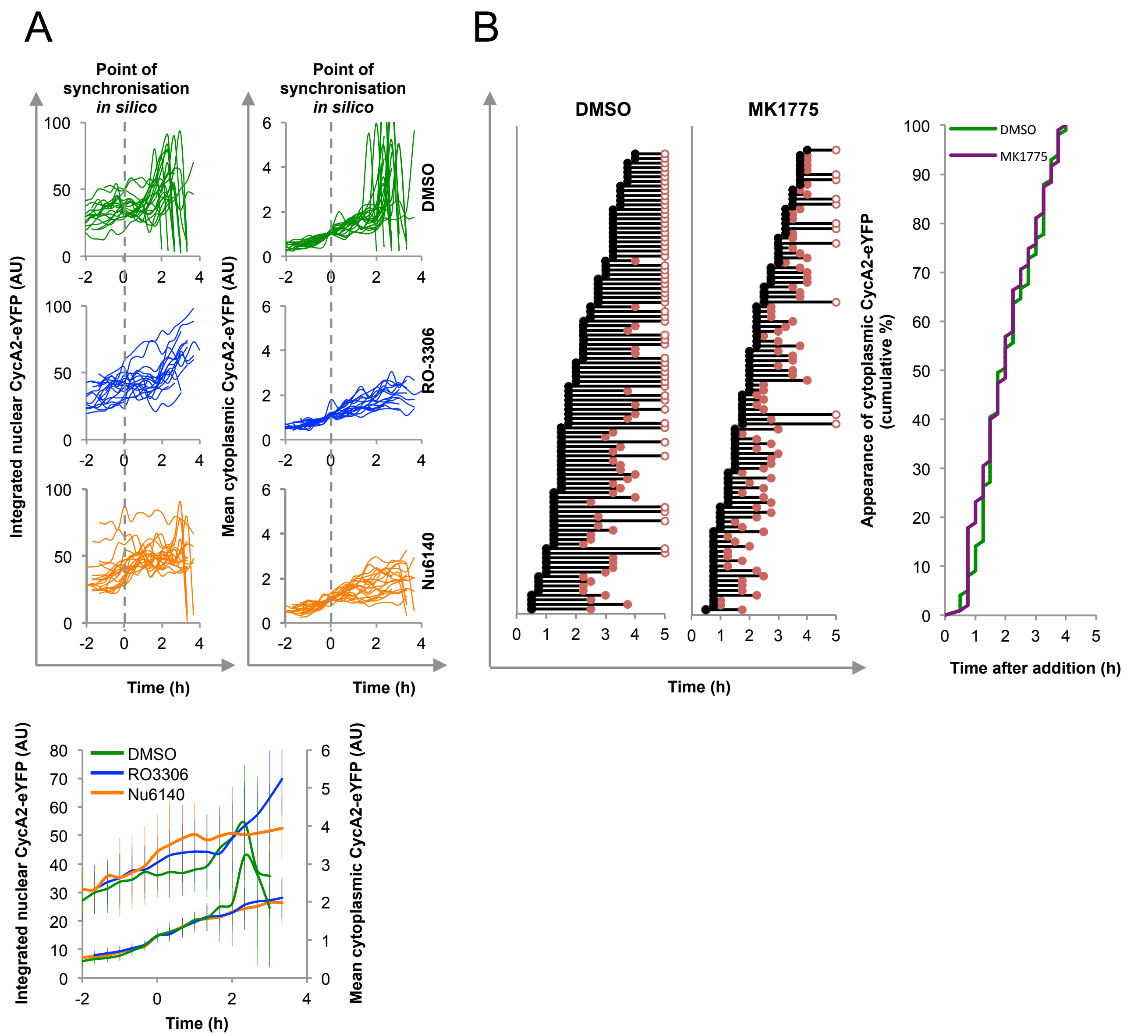

Supplementary Figure 3

A

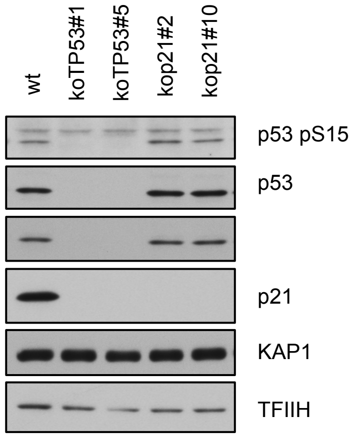

B

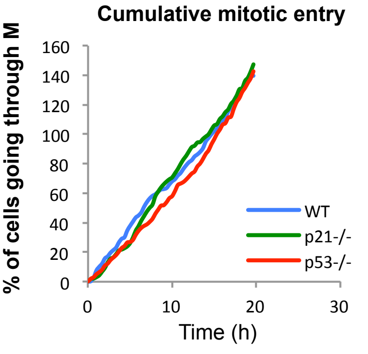

Supplementary Figure 4